

# Suppression of antiferromagnetic correlations by quenched dipole–type impurities

V. Cherepanov, I. Ya. Korenblit, Amnon Aharony, and O. Entin-Wohlman  
*School of Physics and Astronomy, Raymond and Beverly Sackler Faculty of Exact Sciences,  
Tel Aviv University, Tel Aviv 69978, Israel*

(March 1, 2018)

## Abstract

The effect of quenched random ferromagnetic bonds on the antiferromagnetic correlation length,  $\xi_{2D}$ , of a two–dimensional Heisneberg model is studied, applying the renormalization group method to the classical non–linear sigma model with quenched random dipole moments. It is found that the antiferromagnetic long range order is destroyed for any non–zero concentration,  $x$ , of the dipolar defects, even at zero temperature. Below a line  $T \propto x$ , where  $T$  is the temperature,  $\xi_{2D}$  is independent of  $T$ , and decreases exponentially with  $x$ . At higher temperatures, it decays exponentially with  $\rho_s^{\text{eff}}/T$ , with an effective stiffness constant  $\rho_s^{\text{eff}}$ , which decreases with  $x/T$ . The results are used to estimate the three–dimensional Néel temperature, which decays linearly with  $x$  at small concentrations, and drops precipitously at a critical concentration. These predictions are compared with experiments on doped copper oxides, and are shown to reproduce successfully some of the prominent features of the data.

75.10.-b, 75.10.Nr, 75.50.Ee

Typeset using REVTeX

## I. INTRODUCTION

Consider a Heisenberg antiferromagnet, with a concentration  $x$  of quenched random nearest neighbor ferromagnetic (FM) bonds. These bonds compete with the antiferromagnetic (AFM) order, and introduce frustration into the problem. If the FM exchange on the “impurity” bonds is sufficiently strong, then the two spins at the end of each such bond prefer energetically to be parallel to each other, and perpendicular to the background AFM staggered moment. The staggered moments on the other sites then cant in this perpendicular direction, and at large distance this canting angle decays with distance  $r$  as  $1/r^{d-1}$  in  $d$  dimensions, similarly to the decay of magnetic moments in the presence of a magnetic dipole. [1] This follows from a mapping of the low temperature equations for the spin configuration at the minimal energy onto the Laplace equation. At sufficiently low  $d$  such impurities destroy the AFM long range order at all finite temperatures  $T$ , giving rise to a spin glass like phase. [2] The present paper presents a renormalization group (RG) analysis of the AFM correlations in the presence of such quenched randomness. As we show, this complex random problem is exactly renormalizable in two dimensions (2D), allowing a detailed study of the dependence of the 2D AFM correlation length  $\xi_{2D}$  on  $T$  and on  $x$ . This also allows an  $\epsilon$ -expansion in  $d = 2 + \epsilon$  dimensions. The three dimensional Néel temperature  $T_N(x)$  of lamellar system is estimated by a model of weakly coupled planes.

It is hoped that our model can describe the  $T - x$  phase diagram of various antiferromagnets with random FM bonds. One motivation of the present study arises from its possible relevance to the understanding of the doping dependence of the magnetic order in the lamellar copper oxides. Experimentally, doping such oxides leads to a rapid decrease in both  $\xi_{2D}$  and  $T_N$ . [3–10] Experiments on doped  $\text{La}_2\text{CuO}_4$  show that above  $x = x_c \approx 2\%$   $\xi_{2D}$  remains finite even at zero temperature, and there is no AFM order. This strong effect of the doping has been attributed to frustration, due to strong FM exchange on the Cu–O–Cu

bonds which have localized holes due to the doping. [2] This frustration was also predicted to yield a magnetic spin glass phase for  $x > x_c$ , [2] as recently confirmed in detail in doped  $\text{La}_2\text{CuO}_4$ . [11] The experimental verification of this spin freezing above  $x_c$  [4,8,10–13] confirms the picture of *localized* holes. This localization is also confirmed by direct conductance measurements at  $x \leq 5\%$  and low temperature  $T$ . [4,12]

The description of doped lamellar cuprates by quenched FM bonds requires several assumptions, which will be discussed in detail below. In particular, at high temperature  $T$  the “dipolar” moments which describe the dopant bonds may fluctuate, turning this aspect of the problem into one which requires a combined annealed and quenched averaging. Indeed, Glazman and Ioselevich (GI) [14] studied this problem in its annealed limit, and calculated  $\xi_{2D}$  to leading order in  $x/T$  (See also Ref. [15].) Although the locations  $\mathbf{r}_\ell$  of the dipole-like impurities are randomly *quenched*, each impurity involves an effective dipole moment  $\mathbf{m}(\mathbf{r}_\ell)$  which is still free to reach *annealed* equilibrium in the presence of all the other dipoles. At low temperature, these moments freeze as in a dipole glass. However, unlike the dipole glass, where the interactions are fixed, the interactions among the dipoles are mediated by the AFM spin background, whose behavior also depends on temperature, concentration and configuration of the dipole moments. In the absence of a simple systematic way to handle such a combined quenched–annealed problem, GI stopped their explicit calculations at the low- $x$  expansion. Here we argue that at sufficiently low  $T$  the dipole moments, which interact via randomly quenched dipole–dipole interactions, freeze in a random spin glassy way. [16,17] At low temperatures we thus compare the experiments with our quenched theory. The actual fitting of data from the cuprates should involve some interpolation between the annealed and quenched limits. As we show, the annealed and quenched calculations coincide to leading order in  $x/T$ , and therefore our quenched results supply a good interpolation over the whole range. Other assumptions, concerning e. g. the mobility of the holes forming the dopant bonds, will be discussed below. In any case, our model should give a good description of the lamellar cuprates at low  $T$ , and should describe other lamellar antiferromagnets doped with FM bonds.

A second major motivation concerns the fact that, as we show below, the quenched random dipoles are coupled to the gradient of the order parameter, and therefore they are equivalent to correlated random fields, whose correlations in momentum space are proportional to the square of the momentum. Such fields lower the critical dimensions of the random field  $\mathcal{N}$ -component spin model by 2, from 6 to 4 for the upper critical dimension, and from 4 to 2 for the lower one. In Ref. [18] this has been established for the limit  $\mathcal{N} \rightarrow \infty$ . Here we show that the lower critical dimension is shifted down from  $d = 4$  to  $d = 2$ , for all  $\mathcal{N} > 2$ . As a result, both the temperature and the variance of the random dipole moments (which is proportional to the concentration,  $x$ ) are marginal (in the RG sense) at  $d = 2$ , allowing for an analytical solution of the recursion relations. This marginality of the randomness is related to the 2D infrared divergence of the Villain canted states. [1] Within the one-loop approximation, we obtain an exact expression for the exponential part of the 2D correlation length, which remains finite at all non-zero  $x$ .

We describe the system by the reduced Hamiltonian (i.e., the Hamiltonian divided by the temperature  $T$ )

$$\mathcal{H} = \mathcal{H}_{\text{pure}} + \mathcal{H}_{\text{int}}, \quad (1)$$

where  $\mathcal{H}_{\text{pure}}$  is the classical non-linear sigma model (NL $\sigma$ M) for the pure (non-random) system, representing the long wave length Hamiltonian related to the fluctuations of the unit vector  $\mathbf{n}(\mathbf{r})$  of antiferromagnetism,

$$\mathcal{H}_{\text{pure}} = \frac{1}{2t} \int d\mathbf{r} \sum_{i,\mu} (\partial_i n_\mu)^2, \quad t = T/\rho_s. \quad (2)$$

Here  $i = 1, \dots, d$  and  $\mu = 1, \dots, \mathcal{N}$  run over the spatial Cartesian components and over the spin components, respectively,  $\rho_s$  is the stiffness constant and  $\partial_i \equiv \partial/\partial x_i$ . This Hamiltonian is known to give an excellent description of the undoped antiferromagnet, both theoretically [19] and experimentally [4]. The success of this description results from the fact that, although the problem involves quantum spin fluctuations, these can be integrated out at any finite  $T$ , causing only a renormalization of  $\rho_s$ .

$\mathcal{H}_{\text{int}}$  is constructed [14] to reproduce the dipolar effects at long distances: Denoting by  $\mathbf{a}(\mathbf{r}_\ell)$  the unit vector directed along the doped bond at  $\mathbf{r}_\ell$ , and by  $M\mathbf{m}(\mathbf{r}_\ell)$  the corresponding dipole moment (where  $\mathbf{m}(\mathbf{r}_\ell)$  is a unit vector giving the direction of the dipole, and  $M$  is its magnitude),

$$\mathcal{H}_{\text{int}} = \frac{1}{t} \int d\mathbf{r} \sum_i \mathbf{f}_i(\mathbf{r}) \cdot \partial_i \mathbf{n}, \quad (3)$$

with

$$\mathbf{f}_i(\mathbf{r}) = M \sum_\ell \delta(\mathbf{r} - \mathbf{r}_\ell) a_i(\mathbf{r}_\ell) \mathbf{m}(\mathbf{r}_\ell). \quad (4)$$

Note that since  $\mathbf{n}$  is a unit vector,  $\partial_i \mathbf{n}$  is perpendicular to  $\mathbf{n}$  and hence  $\mathcal{H}_{\text{int}}$  contains only the  $\mathcal{N} - 1$  components of the  $\mathcal{N}$ -component vector  $\mathbf{f}_i$  which are transverse to  $\mathbf{n}$ . However, since the vector  $\mathbf{n}$  varies with  $\mathbf{r}$ , all the components of  $\mathbf{m}$  may enter at the end. As stated, GI treated the variables  $\mathbf{m}$  as annealed. Here we treat all the variables  $\mathbf{r}_\ell$ ,  $\mathbf{a}(\mathbf{r}_\ell)$ , and  $\mathbf{m}(\mathbf{r}_\ell)$  as quenched. Denoting quenched averages by [...], we write

$$\begin{aligned} [\mathbf{a}(\mathbf{r})] &= 0, \\ [m_\mu(\mathbf{r})] &= 0, \\ [a_i(\mathbf{r})a_j(\mathbf{r}')] &= \delta_{ij}\delta(\mathbf{r} - \mathbf{r}')x/d, \\ [m_\mu(\mathbf{r})m_\nu(\mathbf{r}')] &= Q\delta_{\mu\nu}\delta(\mathbf{r} - \mathbf{r}'), \end{aligned} \quad (5)$$

so that  $[f_{i\mu}] = 0$  and

$$[f_{i\mu}(\mathbf{r})f_{j\nu}(\mathbf{r}')] = \lambda\delta_{\mu\nu}\delta_{ij}\delta(\mathbf{r} - \mathbf{r}'), \quad (6)$$

with

$$\lambda = M^2 Q x / d \equiv Ax, \quad (7)$$

where  $A = \mathcal{O}(1)$ . At low  $T$  one expects  $Q \approx 1/\mathcal{N}$ .

One can see now that  $\mathcal{H}_{\text{int}}$  represents random fields with quenched correlations: Fourier transforming the variables in Eq. (3),  $\mathcal{H}_{\text{int}}$  can be written in the form

$$\mathcal{H}_{\text{int}} = \frac{1}{(2\pi)^{dt}} \int d\mathbf{k} \sum_{\mu} h_{\mu}(\mathbf{k}) n_{\mu}(-\mathbf{k}), \quad (8)$$

with the random field  $\mathbf{h}(\mathbf{k})$ ,

$$h_{\mu}(\mathbf{k}) = i \sum_j k_j \int d\mathbf{r} f_{j\mu}(\mathbf{r}) e^{i\mathbf{k}\cdot\mathbf{r}}, \quad (9)$$

which has quenched correlations

$$[h_{\mu}(\mathbf{k}) h_{\nu}^*(\mathbf{k}')] = \lambda k^2 \delta_{\mu\nu} \delta(\mathbf{k} - \mathbf{k}'). \quad (10)$$

Such correlations shift the critical dimension of the random field Heisenberg problem down to 2. A heuristic way to show this follows Imry and Ma [20] in assuming an ordered state and considering the transverse spin fluctuations,  $\mathcal{M}^{\perp}(\mathbf{r})$ . In momentum space,  $\mathcal{M}^{\perp}(\mathbf{q}) = G^{\perp}(\mathbf{q}) h^{\perp}(\mathbf{q})$ , with  $G^{\perp}(\mathbf{q}) \sim 1/q^2$ , and  $h^{\perp}(\mathbf{q})$  denoting the transverse random field. Thus

$$\begin{aligned} [\mathcal{M}^{\perp}(\mathbf{r}) \mathcal{M}^{\perp}(\mathbf{r}')] &= \left(\frac{1}{2\pi}\right)^{2d} \int d^d q d^d q' \times \\ G^{\perp}(\mathbf{q}) G^{\perp}(\mathbf{q}') [h^{\perp}(\mathbf{q}) h^{\perp}(\mathbf{q}')] &e^{i(\mathbf{q}\cdot\mathbf{r} + \mathbf{q}'\cdot\mathbf{r}')} \end{aligned} \quad (11)$$

For  $[h_{\mu}(\mathbf{q}) h_{\nu}(\mathbf{q}')] \propto \delta_{\mu\nu} q^{\theta} \delta(\mathbf{q} + \mathbf{q}')$ , this integral diverges for  $d < 4 - \theta$ , implying that the assumption of long range order is invalid. This identifies the lower critical dimension as  $d_{\ell} = 4 - \theta$ , and for our case,  $d_{\ell} = 2$ . The calculations below support this picture. In addition to giving an exact solution for the problem at hand, we note that the present formalism might also be used as a starting point for a double expansion, in  $\epsilon$  and in  $2 - \theta$ , aiming at other random field problems.

The conventional method to treat the NL $\sigma$ M expands the order parameter unit vector  $\mathbf{n}$  about a spatially uniform ordered state. [21,22] Using replicas to handle the quenched randomness we have found that this approach generated local random fields, which seem to break the symmetries of the original model. Similar problems were found for other problems near 4D, where they required a resummation of the perturbation expansion. [23] In our case, the problems may have come either from the replicas or from the assumption of a spatially uniform state. Such a state does not exist when there is some local freezing of the moments

in random directions (as happens in the random case discussed here). We avoid both of these by going back to the original RG approach by Polyakov, [24] and by treating the randomness without replicas. In 2D, this allows us to obtain  $\xi_{2D}$  for all values of  $\rho_s x/T$ .

We show that the quenched dipoles suppress the antiferromagnetic correlations, so that the correlation length is a decreasing function of  $\rho_s x/T$ , remaining finite at any non-zero  $x$ , even at  $T = 0$ . This implies the destruction of the antiferromagnetic long range order in 2D for any concentration. As  $x$  increases,  $\xi_{2D}(T = 0)$  decays exponentially, representing the sizes of the Imry-Ma domains for this system.

In order to compare the results of our model with experiments performed on doped lamellar cuprates, we consider the 3D ordering of a system of weakly coupled planes by using the relation  $\alpha \xi_{2D}^2 \sim 1$ . Here,  $\alpha$  represents either the interplane coupling, that is the relative interplane exchange,  $J_{\perp}/J \sim J_{\perp}/2\pi\rho_s$ , or the in-plane relative spin anisotropy (in the presence of which even an infinitesimal coupling suffices to yield 3D ordering). Although it is not expected to give the correct 3D critical behavior, this procedure proved to give excellent results for the 3D Néel temperature in the pure case. [4] This “mean field” procedure is also justified by an RG argument: to linear order in  $\alpha$ , the RG recursion relation for  $\alpha$  is  $\alpha' = e^{2\ell}\alpha$ , where  $e^{\ell}$  is the length rescale factor. After  $\ell$  iterations of the RG the effective coupling between planes involves renormalized spins, contained in the area  $e^{2\ell}$  of the renormalized cell. A 3D behavior is expected when this effective coupling becomes comparable to 1. As we show in Appendix B, similar results for the phase diagram are also found from integrating the RG recursion relations in  $d = 2 + \epsilon$  dimensions. We obtain an explicit form for  $T_N(x)$ , and compare it in detail with available data. Our results reproduce prominent features of the observed phase diagram, in particular the fast decrease of the Néel temperature with increasing  $x$  and the disappearance of the 3D long range order at  $x \sim 2\%$ .

The outline of the paper is as follows. Section II discusses the RG procedure, and Sec. III describes the RG recursion relations for the quenched averaging. The 2D recursion relations are then solved in Sec. IV, and the resulting  $\xi_{2D}$  is used for estimating the 3D phase transition line  $T_N(x)$  in Sec. V. Section VI then contains a discussion of the alternative

annealed averaging. The results are compared with experiments on doped cuprates in Sec. VII, and discussed in Sec. VIII. Details of the calculations and extensions to  $d = 2 + \epsilon$  are given in the Appendices.

## II. THE RENORMALIZATION GROUP PROCEDURE

Following the RG approach of Polyakov, [24,25] we decompose  $\mathbf{n}(\mathbf{r})$  into a slowly varying part, given by the unit vector  $\tilde{\mathbf{n}}(\mathbf{r})$ , and  $\mathcal{N} - 1$  fast variables  $\phi_\mu(\mathbf{r})$ , such that

$$\begin{aligned}\mathbf{n}(\mathbf{r}) &= \tilde{\mathbf{n}}(\mathbf{r})\sqrt{1 - \phi^2(\mathbf{r})} + \sum_{\mu=1}^{\mathcal{N}-1} \phi_\mu(\mathbf{r})\mathbf{e}_\mu(\mathbf{r}), \\ \phi^2(\mathbf{r}) &= \sum_{\mu=1}^{\mathcal{N}-1} \phi_\mu^2(\mathbf{r}).\end{aligned}\tag{12}$$

The unit vectors  $\tilde{\mathbf{n}}(\mathbf{r})$  and  $\mathbf{e}_\mu(\mathbf{r})$ ,  $\mu = 1, \dots, \mathcal{N} - 1$ , form an orthonormal basis. The Fourier transform of the fast variables  $\phi_\mu$ ,

$$\phi_\mu(\mathbf{r}) = (2\pi)^{-d} \int d\mathbf{q} e^{i\mathbf{q}\mathbf{r}} \phi_\mu(\mathbf{q}),\tag{13}$$

is restricted to wave vectors  $\mathbf{q}$  in the range  $b^{-1} \leq q \leq 1$ . The upper bound is the inverse of the microscopic length (which is measured in units of the lattice constant), and  $b$  is the length rescale factor for the renormalization procedure. These  $q$  values are to be integrated out. After the iteration the correlation length  $\xi$  is renormalized into  $\xi/b$ .

The Hamiltonian  $\mathcal{H}$  requires the derivatives of  $\mathbf{n}(\mathbf{r})$ . Using the relations  $\tilde{\mathbf{n}} \cdot \partial_i \tilde{\mathbf{n}} = 0$ ,  $\tilde{\mathbf{n}} \cdot \mathbf{e}_\mu = 0$ , and  $\mathbf{e}_\mu \cdot \mathbf{e}_\nu = \delta_{\mu\nu}$ , we set

$$\partial_i \tilde{\mathbf{n}} = \sum_{\mu=1}^{\mathcal{N}-1} B_i^\mu \mathbf{e}_\mu, \quad \partial_i \mathbf{e}_\mu = \sum_{\nu=1}^{\mathcal{N}-1} A_i^{\mu\nu} \mathbf{e}_\nu - B_i^\mu \tilde{\mathbf{n}},\tag{14}$$

where  $A_i^{\nu\mu} = \mathbf{e}_\mu \cdot \partial_i \mathbf{e}_\nu = -A_i^{\mu\nu}$ . Then we find

$$\begin{aligned}\partial_i \mathbf{n} &= \tilde{\mathbf{n}} \left\{ \partial_i \sqrt{1 - \phi^2} - \sum_{\mu=1}^{\mathcal{N}-1} B_i^\mu \phi_\mu \right\} \\ &+ \sum_{\mu=1}^{\mathcal{N}-1} \mathbf{e}_\mu \left\{ \partial_i \phi_\mu + B_i^\mu \sqrt{1 - \phi^2} + \sum_{\nu=1}^{\mathcal{N}-1} A_i^{\nu\mu} \phi_\nu \right\}.\end{aligned}\tag{15}$$



We show in Appendix A that the functions  $A_i^{\mu\nu}$ , which give the first derivatives of the base vectors  $\mathbf{e}_\mu$ , can be eliminated by a suitable gauge transformation when one ignores higher order derivatives. [24,26] Therefore, these are omitted in the following.

In terms of the new variables, the Hamiltonian  $\mathcal{H}$ , to order  $\phi_\mu^2$ , reads

$$\mathcal{H} = \mathcal{H}_0 + \mathcal{H}_1 + \mathcal{H}_2 + \mathcal{H}_3 + \mathcal{H}_4, \quad (16)$$

with

$$\mathcal{H}_0 = \frac{1}{2t} \int d\mathbf{r} \sum_{i\mu} \left\{ (B_i^\mu(\mathbf{r}))^2 + (\partial_i \phi_\mu(\mathbf{r}))^2 \right\}, \quad (17)$$

$$\mathcal{H}_1 = \frac{1}{t} \int d\mathbf{r} \sum_{i\mu} B_i^\mu(\mathbf{r}) g_i^\mu(\mathbf{r}), \quad (18)$$

$$\mathcal{H}_2 = \frac{1}{2t} \int d\mathbf{r} \sum_{i\nu\mu} B_i^\mu(\mathbf{r}) B_i^\nu(\mathbf{r}) \{ \phi_\mu(\mathbf{r}) \phi_\nu(\mathbf{r}) - \delta_{\mu\nu} \phi^2(\mathbf{r}) \}, \quad (19)$$

$$\mathcal{H}_3 = -\frac{1}{t} \int d\mathbf{r} \sum_{i\mu} B_i^\mu(\mathbf{r}) \left\{ u_i(\mathbf{r}) \phi_\mu(\mathbf{r}) + \frac{1}{2} g_i^\mu(\mathbf{r}) \phi^2 \right\}, \quad (20)$$

and

$$\mathcal{H}_4 = \frac{1}{t} \int d\mathbf{r} \sum_{i\mu} \left\{ g_i^\mu(\mathbf{r}) \partial_i \phi_\mu(\mathbf{r}) - \frac{1}{2} u_i(\mathbf{r}) \partial_i \phi_\mu^2(\mathbf{r}) \right\}. \quad (21)$$

Here we have introduced the notations

$$u_i(\mathbf{r}) = \tilde{\mathbf{n}}(\mathbf{r}) \cdot \mathbf{f}_i(\mathbf{r}), \quad g_i^\mu(\mathbf{r}) = \mathbf{e}_\mu(\mathbf{r}) \cdot \mathbf{f}_i(\mathbf{r}), \quad (22)$$

for the longitudinal and transverse components, respectively, of  $\mathbf{f}_i$  in the new variables. Indeed, Eq. (18) represents the bare form of  $\mathcal{H}_{\text{int}}$  in this system. In  $\mathcal{H}_0$  the slow variables,  $B_i^\mu$ , are separated from the fast ones  $\phi_\mu$ . [One should notice that  $(\partial_i n_\mu)^2$  also yields the contribution  $(1/t) \int d\mathbf{r} \sum_{i\mu} B_i^\mu \partial_i \phi_\mu$ . However, this term vanishes upon Fourier transforming, as  $\phi_\mu$  pertains to the large  $q$  portion of the Brillouin zone, while the slow variables  $B_i^\mu$  belong to the small  $q$  values,  $q \leq b^{-1}$ .] The Hamiltonians  $\mathcal{H}_2$ ,  $\mathcal{H}_3$ , and  $\mathcal{H}_4$ , of order  $\mathcal{O}(B^2)$ ,  $\mathcal{O}(B^1)$ , and  $\mathcal{O}(B^0)$ , respectively, will be treated in perturbation theory.

### III. RENORMALIZATION GROUP EQUATIONS

The first step in deriving the recursion relations involves integration over the fast variables  $\phi_\mu$ . This requires the Green's functions,

$$\begin{aligned} \langle \phi_\mu(\mathbf{r})\phi_\nu(\mathbf{r}') \rangle &= \delta_{\mu\nu}G(\mathbf{r} - \mathbf{r}'), \\ G(\mathbf{r}) &= (2\pi)^{-d} \int_{b^{-1} \leq q \leq 1} d\mathbf{q} e^{i\mathbf{q}\cdot\mathbf{r}} \hat{G}(q), \quad \hat{G}(q) = t/q^2, \end{aligned} \quad (23)$$

where  $\langle \dots \rangle$  denotes a thermal average with  $\mathcal{H}_0$ . As we shall see below, to leading order in  $\epsilon = d - 2$  we need  $G(r)$  only at strictly 2D, where

$$G(0) = \frac{t}{2\pi} \ln b. \quad (24)$$

Hence  $\langle \phi^2 \rangle$  is small for  $\ln b \ll 2\pi/t$ . In practice,  $G(r)$  is significantly different from zero only for  $1 < r < b$ , where it is approximately given by the 2D Coulomb interaction

$$G(r) \approx \frac{t}{2\pi} \ln \frac{b}{r}. \quad (25)$$

We next turn to the perturbation expansion in  $\mathcal{H}_2$ ,  $\mathcal{H}_3$ , and  $\mathcal{H}_4$ . The first order yields

$$\begin{aligned} \mathcal{H}^{(1)} = \langle \mathcal{H}_2 + \mathcal{H}_3 \rangle &= \frac{1}{2t} \int d\mathbf{r} \sum_{i\mu} (B_i^\mu(\mathbf{r}))^2 (2 - \mathcal{N}) G(0) \\ &\quad - \frac{1}{2t} \int d\mathbf{r} \sum_{i\mu} B_i^\mu(\mathbf{r}) g_i^\mu(\mathbf{r}) (\mathcal{N} - 1) G(0). \end{aligned} \quad (26)$$

The first term here represents the leading order renormalization of  $1/t$ , as usual. [22,24] The second term, which is linear in  $B_i^\mu$ , is similar to the initial  $\mathcal{H}_{\text{int}}$ , or to the equivalent Eq. (18). In fact, this term contributes to the renormalization of the transverse components of  $\mathbf{f}_i$ .

Higher order perturbations contain higher powers of  $\phi$ , which yield higher powers of  $G$  and hence of  $t$ . In the following, we keep only leading powers of  $t$ . Neglecting the terms involving products of two  $G$ 's, the second order perturbation yields

$$\mathcal{H}^{(2)} = -\frac{1}{2} \langle (\mathcal{H}_3 + \mathcal{H}_4)^2 \rangle =$$

$$\begin{aligned}
& - \frac{1}{2t^2} \int d\mathbf{r}_1 d\mathbf{r}_2 \sum_{ij\mu} g_i^\mu(\mathbf{r}_1) g_j^\mu(\mathbf{r}_2) \partial_{1i} \partial_{2j} G(\mathbf{r}_{12}) \\
& + \frac{1}{t^2} \int d\mathbf{r}_1 d\mathbf{r}_2 \sum_{ij\mu} B_i^\mu(\mathbf{r}_1) u_i(\mathbf{r}_1) g_j^\mu(\mathbf{r}_2) \partial_{2j} G(\mathbf{r}_{12}) \\
& - \frac{1}{2t^2} \int d\mathbf{r}_1 d\mathbf{r}_2 \sum_{ij\mu} B_i^\mu(\mathbf{r}_1) B_j^\mu(\mathbf{r}_2) u_i(\mathbf{r}_1) u_j(\mathbf{r}_2) G(\mathbf{r}_{12}), \\
& \mathbf{r}_{12} = \mathbf{r}_1 - \mathbf{r}_2.
\end{aligned} \tag{27}$$

The first term here is  $B$ -independent. In principle, it gives rise to an interaction between the dipoles: Inserting  $G(\mathbf{r})$  and the explicit expressions for  $g_i^\mu$  [Eqs. (4) and (22)] we rewrite this term in the form

$$\mathcal{H}_{\text{dd}} = \frac{1}{t} \sum_{k\ell} I_{k\ell} \mathbf{m}_\perp(\mathbf{r}_k) \cdot \mathbf{m}_\perp(\mathbf{r}_\ell), \tag{28}$$

where  $\mathbf{m}_\perp(\mathbf{r}_\ell)$  is the component of the dipole moment at  $\mathbf{r}_\ell$  which is perpendicular to  $\tilde{\mathbf{n}}$ , and

$$\begin{aligned}
I_{k\ell} = & \frac{1}{4\pi} M^2 \frac{1}{r_{k\ell}^d} \times \\
& \left\{ 2 \frac{(\mathbf{a}(\mathbf{r}_k) \cdot \mathbf{r}_{k\ell})(\mathbf{a}(\mathbf{r}_\ell) \cdot \mathbf{r}_{k\ell})}{r_{k\ell}^2} - \mathbf{a}(\mathbf{r}_k) \cdot \mathbf{a}(\mathbf{r}_\ell) \right\},
\end{aligned} \tag{29}$$

with  $r_{k\ell} < b$ . Apart from trivial factors, this reproduces the effective dipole–dipole interaction found in Ref. [14]. There, Eq. (28) was used to integrate over the variables  $\mathbf{m}_\perp$ , treating them as annealed variables. In the present calculation we treat the dipoles as quenched, and therefore Eq. (28) simply represents an additional constant to the energy. We return to this point in the following. The other two ( $B$ -dependent) terms in the second order perturbation Hamiltonian, Eq. (27), will contribute to the renormalization of the temperature and the variance of the dipolar quenched interaction.

Finally, the third order perturbation Hamiltonian, keeping terms up to order  $B^2$ , is

$$\mathcal{H}^{(3)} = \frac{1}{6} \langle \mathcal{H}_4^3 \rangle + \frac{1}{2} \left( \langle \mathcal{H}_4^2 \mathcal{H}_3 \rangle + \langle \mathcal{H}_4 \mathcal{H}_3^2 \rangle + \langle \mathcal{H}_2 \mathcal{H}_4^2 \rangle \right). \tag{30}$$

Integrating out the variables  $\phi$ , it is seen that the first term here is independent of  $B$ ; it contributes further to the dipole–dipole interaction. The next term in (30) yields an expression linear in  $B$ ,

$$\begin{aligned}
\frac{1}{2}\langle \mathcal{H}_4^2 \mathcal{H}_3 \rangle &= -\frac{1}{2t^3} \int d\mathbf{r}_1 d\mathbf{r}_2 d\mathbf{r}_3 \sum_{ijk} \sum_{\mu} B_i^{\mu}(\mathbf{r}_1) \times \\
&\left\{ \sum_{\nu} g_i^{\mu}(\mathbf{r}_1) g_j^{\nu}(\mathbf{r}_2) g_k^{\nu}(\mathbf{r}_3) \partial_{2j} \partial_{3k} G(\mathbf{r}_{21}) G(\mathbf{r}_{31}) \right. \\
&\left. - 2u_i(\mathbf{r}_1) g_j^{\mu}(\mathbf{r}_2) u_k(\mathbf{r}_3) \partial_{2j} \partial_{3k} G(\mathbf{r}_{23}) G(\mathbf{r}_{31}) \right\}, \tag{31}
\end{aligned}$$

which again contributes to  $\mathcal{H}_{\text{int}}$ , while the last term there gives a  $B^2$  contribution

$$\begin{aligned}
\frac{1}{2}\langle \mathcal{H}_4 \mathcal{H}_3^2 + \mathcal{H}_2 \mathcal{H}_4^2 \rangle &= \frac{1}{2t^3} \int d\mathbf{r}_1 d\mathbf{r}_2 d\mathbf{r}_3 \sum_{ijk} \sum_{\mu} \times \\
&\left\{ -B_i^{\mu}(\mathbf{r}_1) B_i^{\mu}(\mathbf{r}_2) u_i(\mathbf{r}_1) u_j(\mathbf{r}_2) u_k(\mathbf{r}_3) \partial_{3k} G(\mathbf{r}_{13}) G(\mathbf{r}_{23}) \right. \\
&+ 2 \sum_{\nu} B_i^{\mu}(\mathbf{r}_1) B_j^{\nu}(\mathbf{r}_2) u_i(\mathbf{r}_1) g_j^{\nu}(\mathbf{r}_2) g_k^{\mu}(\mathbf{r}_3) \partial_{3k} G(\mathbf{r}_{12}) G(\mathbf{r}_{23}) \\
&+ \sum_{\nu} (B_i^{\mu}(\mathbf{r}_1) B_i^{\nu}(\mathbf{r}_1) g_j^{\mu}(\mathbf{r}_2) g_k^{\nu}(\mathbf{r}_3) - \\
&\left. B_i^{\mu}(\mathbf{r}_1) B_i^{\mu}(\mathbf{r}_1) g_j^{\nu}(\mathbf{r}_2) g_k^{\nu}(\mathbf{r}_3)) \partial_{2j} \partial_{3k} G(\mathbf{r}_{12}) G(\mathbf{r}_{13}) \right\}. \tag{32}
\end{aligned}$$

Except for the first term in Eq. (26), all the generated terms involve the longitudinal and transverse components of the vectors  $\mathbf{f}_i$ ,  $u_i$  and  $g_i^{\mu}$ , Eq. (22), which depend on the quenched random variables  $\mathbf{r}_{\ell}$ ,  $\mathbf{a}(\mathbf{r}_{\ell})$ , and  $\mathbf{m}(\mathbf{r}_{\ell})$ . Using Eq. (6) we thus find

$$\begin{aligned}
[g_i^{\mu}(\mathbf{r}) g_j^{\nu}(\mathbf{r}')] &= \lambda \delta_{ij} \delta_{\mu\nu} \delta(\mathbf{r} - \mathbf{r}'), \\
[u_i(\mathbf{r}) u_j(\mathbf{r}')] &= \lambda \delta_{ij} \delta(\mathbf{r} - \mathbf{r}'), \\
[u_i(\mathbf{r}) g_j^{\mu}(\mathbf{r}')] &= 0. \tag{33}
\end{aligned}$$

We now obtain the recursion relations of the RG. Consider first the quenched averages of the integrated Hamiltonians  $\mathcal{H}^{(\ell)}$ ,  $\ell = 1, 2, 3$ . This will constitute the renormalization of  $1/t$ . Rescaling the lengths by  $b^{-1}$  and the slow derivatives  $B_i^{\mu}(\mathbf{q})$  by  $b^{d-1}$ , the new temperature prefactor, multiplying the integral over  $(B_i^{\mu})^2$ , obeys the RG equation

$$\frac{1}{t'} = b^{d-2} \left[ \frac{1}{t} + \frac{2 - \mathcal{N}}{2\pi} \ln b + \frac{1 - \mathcal{N}}{2\pi} \frac{\lambda}{t} \ln b \right], \tag{34}$$

which is valid to first order in  $\epsilon = d - 2$ ,  $t$  and  $\lambda$ . To obtain this equation, we have used Eqs. (33) and the relation

$$\sum_j \int d\mathbf{r}_2 (\partial_{2j} G(\mathbf{r}_{12}))^2 = tG(0). \tag{35}$$

The terms in the Hamiltonian linear in  $B_i^\mu$  remain as quenched random contributions. They renormalize  $f_{i\mu}$  and yield a renormalization of its variance  $\lambda$ . To obtain the recursion relation for  $\lambda$ , we collect all terms linear in  $B$  and write them in the form

$$\frac{1}{t} \int d\mathbf{r} \sum_{i\mu} B_i^\mu(\mathbf{r}) \Gamma_i^\mu(\mathbf{r}), \quad (36)$$

with

$$\begin{aligned} \Gamma_i^\mu(\mathbf{r}) = & g_i^\mu(\mathbf{r}) \left(1 - \frac{1}{2}(\mathcal{N} - 1)G(0)\right) \\ & + \frac{1}{t} \int d\mathbf{r}_1 \sum_j u_i(\mathbf{r}) g_j^\mu(\mathbf{r}_1) \partial_{1j} G(\mathbf{r} - \mathbf{r}_1) \\ & - \frac{1}{2t^2} \int d\mathbf{r}_1 d\mathbf{r}_2 \sum_{jk} \times \\ & \left\{ \sum_\nu g_i^\mu(\mathbf{r}) g_j^\nu(\mathbf{r}_1) g_k^\nu(\mathbf{r}_2) \partial_{1j} \partial_{2k} G(\mathbf{r}_1 - \mathbf{r}) G(\mathbf{r}_2 - \mathbf{r}) \right. \\ & \left. - 2u_i(\mathbf{r}) g_j^\mu(\mathbf{r}_1) u_k(\mathbf{r}_2) \partial_{1j} \partial_{2k} G(\mathbf{r}_1 - \mathbf{r}_2) G(\mathbf{r}_2 - \mathbf{r}) \right\}. \end{aligned} \quad (37)$$

We then find the variance of  $\Gamma_i^\mu(\mathbf{r})$  by the one-loop calculation, which to leading order, using Eqs. (33), yields

$$\begin{aligned} \left[ \Gamma_i^\mu(\mathbf{r}) \Gamma_{i'}^{\mu'}(\mathbf{r}') \right] = & \delta_{ii'} \delta_{\mu\mu'} \delta(\mathbf{r} - \mathbf{r}') \times \\ & \lambda \left( 1 - (\mathcal{N} - 1)G(0) + \frac{\lambda}{t} (2 - \mathcal{N})G(0) \right). \end{aligned} \quad (38)$$

Hence, the recursion relation for  $\lambda$  is

$$\left( \frac{\lambda}{t^2} \right)' = b^{d-2} \frac{\lambda}{t^2} \left[ 1 - \frac{t(\mathcal{N} - 1) + \lambda(\mathcal{N} - 2)}{2\pi} \ln b \right]. \quad (39)$$

One also needs to consider the fluctuations of the random terms around their quenched averages, as well as new terms, which were not included in the initial  $\mathcal{H}$ , but are generated by the renormalization procedure. However, these are irrelevant. Let us take as an example the last term in (27), which we may write as

$$\frac{1}{2t} \int d\mathbf{r}_1 d\mathbf{r}_2 \sum_{\mu ij} W_{ij}(\mathbf{r}_1 \mathbf{r}_2) B_i^\mu(\mathbf{r}_1) B_j^\mu(\mathbf{r}_2). \quad (40)$$

Physically, this term describes a random interaction among the gradients of the order parameter  $\mathbf{n}$ , which are absent in the original problem. As the ensemble average contribution of this interaction has been analyzed above, we need to consider here the deviation

$$\begin{aligned} \delta W_{ij}(\mathbf{r}_1 \mathbf{r}_2) = & \\ & -\frac{1}{t} \left[ u_i(\mathbf{r}_1) u_j(\mathbf{r}_2) - \lambda \delta_{ij} \delta(\mathbf{r}_1 - \mathbf{r}_2) \right] G(\mathbf{r}_{12}). \end{aligned} \quad (41)$$

Using Eqs. (33), it is easy to see that

$$\begin{aligned} [\delta W_{ij}(\mathbf{r}_1 \mathbf{r}_2) \delta W_{i'j'}(\mathbf{r}'_1 \mathbf{r}'_2)] = & \\ & \frac{\lambda^2}{t^2} [\delta_{ii'} \delta_{jj'} \delta(\mathbf{r}_1 - \mathbf{r}'_1) \delta(\mathbf{r}_2 - \mathbf{r}'_2) + \\ & \delta_{ij'} \delta_{ji'} \delta(\mathbf{r}_1 - \mathbf{r}'_2) \delta(\mathbf{r}_2 - \mathbf{r}'_1)] G(\mathbf{r}_{12})^2. \end{aligned} \quad (42)$$

Since the range of  $G(\mathbf{r})$  is of order  $b$ , the correlations among these generated  $W$ 's are short range, and in practice the  $W$ 's can be treated as uncorrelated, i.e.

$$\begin{aligned} [\delta W_{ij}(\mathbf{r}_1 \mathbf{r}_2) \delta W_{i'j'}(\mathbf{r}'_1 \mathbf{r}'_2)] = & \\ \Delta [\delta_{ii'} \delta_{jj'} \delta(\mathbf{r}_1 - \mathbf{r}'_1) \delta(\mathbf{r}_2 - \mathbf{r}'_2) + & \\ \delta_{ij'} \delta_{ji'} \delta(\mathbf{r}_1 - \mathbf{r}'_2) \delta(\mathbf{r}_2 - \mathbf{r}'_1)] \delta(\mathbf{r}_{12}). & \end{aligned} \quad (43)$$

A simple power counting then shows that  $(W/t)$  scales as  $b^{2d-2}$ ,  $W$  scales as  $b^d$  and hence

$$\frac{d\Delta}{d\ell} = -d\Delta + O(t, \lambda). \quad (44)$$

Therefore, this generated random coupling is irrelevant. Similar arguments apply for the variances of all the other random terms which are generated in the renormalization procedure.

We now follow standard procedures, and use an infinitesimal length rescale factor  $b = e^{\delta\ell}$ .

To linear order in  $\epsilon = d - 2$ ,  $t$  and  $\lambda$ , Eqs. (34) and (39) now become

$$\begin{aligned} \frac{d}{d\ell} \frac{1}{t} &= \epsilon \frac{1}{t} + \frac{2 - \mathcal{N}}{2\pi} + \frac{1 - \mathcal{N}}{2\pi} \frac{\lambda}{t}, \\ \frac{d}{d\ell} \frac{\lambda}{t^2} &= \epsilon \frac{\lambda}{t^2} + \frac{1 - \mathcal{N}}{2\pi} \frac{\lambda}{t} + \frac{2 - \mathcal{N}}{2\pi} \frac{\lambda^2}{t^2}. \end{aligned} \quad (45)$$

Combining these two equations yields

$$\begin{aligned}\frac{dt}{d\ell} &= -\epsilon t + \frac{\mathcal{N} - 2}{2\pi} t^2 + \frac{\mathcal{N} - 1}{2\pi} t\lambda, \\ \frac{d\lambda}{d\ell} &= -\epsilon\lambda + \frac{\mathcal{N} - 3}{2\pi} \lambda t + \frac{\mathcal{N}}{2\pi} \lambda^2.\end{aligned}\tag{46}$$

As noted above,  $d = 2$  is the lower critical dimension for the NL $\sigma$ M with quenched dipoles. Hence, the 2D problem is exactly renormalizable (as done in the next section), and one can obtain an  $\epsilon$ -expansion in  $d = 2 + \epsilon$  dimensions (as done in Appendix B).

#### IV. THE CORRELATION LENGTH OF A 2D HEISENBERG SYSTEM

We now proceed to calculate  $\xi_{2D}$ . To this end we solve Eqs. (46) with the initial values  $t(\ell_0) \equiv t_0$ , and  $\lambda(\ell_0) \equiv \lambda_0$ . The parameter  $\ell_0$  represents some prefacing iterations. In the simplest case, we assume that  $\ell_0 = 0$ , and thus that  $e^{\ell_0} \equiv L_0 = 1$ . Other choices for  $L_0$  will be discussed below. The solution is particularly simple for the Heisenberg system,  $\mathcal{N} = 3$ . At 2D one finds

$$\begin{aligned}\lambda(\ell) &= \lambda_0 \left(1 - \frac{3\lambda_0}{2\pi} (\ell - \ell_0)\right)^{-1}, \\ \frac{\lambda(\ell)}{t(\ell)} - 1 &= \left(\frac{\lambda(\ell)}{\lambda_0}\right)^{1/3} \left(\frac{\lambda_0}{t_0} - 1\right).\end{aligned}\tag{47}$$

Both  $t(\ell)$  and  $\lambda(\ell)$  flow away from the fixed point  $t = \lambda = 0$  as  $\ell$  increases. From the second of Eqs. (47) it is seen that  $\lambda_0 > t_0$  implies  $\lambda > t$ , and *vice versa*.

The standard scaling relation for the correlation length is

$$\xi(t, \lambda) = e^\ell \xi(t(\ell), \lambda(\ell)).\tag{48}$$

The correlation length  $\xi$  is obtained from the matching condition at  $\ell = \ell^*$ ,

$$\max(t(\ell^*), \lambda(\ell^*)) = 2\pi,\tag{49}$$

where  $\ell^*$  is chosen so that  $\xi(t(\ell^*), \lambda(\ell^*))$  is of the order of the renormalized lattice constant. In practice, this implies that at  $\ell = \ell^*$ ,  $\xi$  is a slowly varying function of its variables, which we denote by  $\tilde{C}(t, \lambda)$ . The first of Eqs. (47) gives

$$\ell^* - \ell_0 = \frac{2\pi}{3\lambda_0} \left(1 - \frac{\lambda_0}{\lambda(\ell^*)}\right), \quad (50)$$

where  $\lambda(\ell^*)$  is equal to  $2\pi$  for  $\lambda_0 > t_0$ , and is given by the solution of

$$\left(\frac{\lambda_0}{\lambda(\ell^*)}\right)^{2/3} \left[\left(\frac{\lambda_0}{\lambda(\ell^*)}\right)^{1/3} - 1 + \frac{\lambda_0}{t_0}\right] = \frac{\lambda_0}{2\pi}, \quad (51)$$

for  $t_0 > \lambda_0$ . Equations (48) and (50) give the 2D correlation length,

$$\xi_{2D}(t, \lambda) = L_0 \tilde{C}(t, \lambda) \exp\left[\frac{2\pi}{3\lambda_0} \left(1 - \frac{\lambda_0}{\lambda(\ell^*)}\right)\right]. \quad (52)$$

In the low temperature limit,  $\lambda_0/t_0 \gg 1$ , we stop iterating when  $\lambda(\ell^*) = 2\pi$ , and consequently

$$\xi_{2D} \approx L_0 \tilde{C}(t, \lambda) \exp\left[\frac{2\pi}{3\lambda_0} \left(1 - \frac{\lambda_0}{2\pi}\right)\right]. \quad (53)$$

It follows that  $\xi_{2D}$  is finite at any finite  $\lambda_0$ , even as  $t_0$  approaches zero. This implies that at zero temperature the long-range order in 2D Heisenberg magnets is destroyed at any small amount of defects (as indeed predicted already by Villain. [1]) This conclusion is also supported by the observation mentioned above, that  $\mathcal{H}_{\text{int}}$  represents correlated random fields. The exponential form of Eq. (53) is similar to that found for other random field problems at the lower critical dimension. [20] Monte Carlo simulations [27] also suggest that the zero temperature correlation length is finite in 2D classical Heisenberg magnets with frustrated bonds. When the correlation length of the 2D system remains finite at zero temperature, it measures the size of the Imry–Ma domains, which is given by an exponential form like Eq. (53).

When  $\lambda_0 < t_0 \ll 1$ , we can approximate  $\lambda_0/\lambda(\ell^*)$  by  $(1 - \lambda_0/t_0)^3$  [see Eq. (51)] and obtain

$$\xi_{2D} = L_0 \tilde{C}(t, \lambda) \exp\left(\frac{2\pi}{t_0} \left[1 - \frac{\lambda_0}{t_0} + \frac{\lambda_0^2}{3t_0^2}\right]\right). \quad (54)$$

The exponential part may be interpreted as a renormalization of the effective stiffness constant in the usual expression for the 2D Heisenberg model,



$$\begin{aligned}\rho_s^{\text{eff}} &= \rho_s(1 - y + y^2/3), \\ y &= \lambda_0/t_0 = Ax\rho_s/T,\end{aligned}\tag{55}$$

where we have used Eq. (7). To leading order in  $x\rho_s/T$ , this coincides with the expression which was obtained in Ref. [14] for an annealed system of dipoles. Indeed, up to the lowest order in  $\lambda/t$  there is no difference between quenched and annealed averaging.

Finally, we discuss the pre-exponential factor in the expressions for the correlation length. For  $\lambda_0 \ll t_0$ , the prefactor  $\tilde{C}(t, \lambda) \approx \tilde{C}(t_0, 0)$  is known: The two-loop [19] and three-loop [28] calculations, based on the quantum NL $\sigma$ M, show that

$$\tilde{C}(t_0, 0) = \frac{e}{8} \frac{c}{2\pi\rho_s} \left(1 - \frac{t_0}{4\pi}\right),\tag{56}$$

where  $c$  is the spin-wave velocity.

At low temperatures, we need the concentration dependence of the pre-exponential factor. This results from higher order loops: At 2D,  $t = 0$  and  $\mathcal{N} = 3$ , the generalized recursion relation for  $\lambda$  has the generic form

$$\frac{d\lambda}{d\ell} = \beta_2\lambda^2 + \beta_3\lambda^3,\tag{57}$$

with  $\beta_2 = 3/(2\pi)$  and with  $\beta_3$  of order  $\beta_2^2$ . The solution for this equation reads

$$\begin{aligned}e^{\ell-\ell_0} &= \left(\frac{\lambda_0(\beta_2 + \beta_3\lambda(\ell))}{\lambda(\ell)(\beta_2 + \beta_3\lambda_0)}\right)^{\beta_3/\beta_2^2} \times \\ &\exp\left[\frac{1}{\beta_2}\left(\frac{1}{\lambda_0} - \frac{1}{\lambda(\ell)}\right)\right],\end{aligned}\tag{58}$$

and therefore, at  $\ell = \ell^*$ , where  $\lambda(\ell^*) = 2\pi$ , we have  $e^{\ell^*} \sim L_0 x^{\beta_3/\beta_2^2} \exp[2\pi/(3\lambda_0)]$ . Consequently,  $\tilde{C}(t, \lambda) \approx \tilde{C}(0, \lambda) \approx C_0\lambda^\omega$ , with  $\omega = \beta_3/\beta_2^2$ .

Within the approximations leading to Eqs. (53) and (54), we note that the expressions in the exponentials and their first derivatives are continuous at  $\lambda_0 = t_0$ , up to terms of order  $\mathcal{O}(\lambda_0/2\pi)$ . In comparing our results with the experiment, we shall use these asymptotic expressions all the way to the line  $\lambda_0 = t_0$ .

## V. THE PHASE BOUNDARY FOR WEAKLY COUPLED PLANES

The 3D transition temperature  $T_N(x)$ , as function of the defect concentration  $x$ , of a system consisting of weakly coupled planes may be deduced from the relation

$$\alpha \xi_{2D}^2(t_N, \lambda) \sim 1. \quad (59)$$

[Note that  $\lambda$  is proportional to  $x$ , cf Eq. (7).] The parameter  $\alpha$  can be generated by an interplane exchange,  $J_\perp/J \sim J_\perp/2\pi\rho_s$ , or some in-plane spin anisotropy. As stated in the Introduction, this procedure gives excellent estimates for  $T_N$ . [4]

To obtain the critical line  $T_N(x)$  we proceed as follows. Using (52) in the relation (59) we find

$$1 - \frac{\lambda_0}{\lambda(\ell^*)} = \frac{3\lambda_0}{4\pi} \ln[\alpha(L_0\tilde{C}(t, \lambda))^2]^{-1}. \quad (60)$$

At low temperature, i.e., for  $\lambda_0 > t_0$ , we have  $\lambda(\ell^*) = 2\pi$  and therefore Eq. (60) is almost independent of  $t$ . It thus yields a critical value for the initial value of the variance,  $\lambda_c$ , and hence a critical concentration,  $x_c$ , above which there is no antiferromagnetic long-range order at any temperature

$$\lambda_c = \frac{2\pi}{1 + \frac{3}{2} \ln[\alpha(L_0\tilde{C}(0, \lambda_c))^2]^{-1}}, \quad (61)$$

with  $\lambda_c = Ax_c$ . In fact,  $\xi_{2D}$  is expected to be practically independent of temperature (except for the very weak dependence of the prefactor  $\tilde{C}$ ) for a range of values,  $\lambda_0 > t_0$ , as given in Eq. (53). Therefore, the critical line  $T_N(x)$  is expected to be practically vertical for  $t_N(x) < \lambda_0 = Ax$ . Below this line, one might expect some range in which spin glass and antiferromagnetism co-exist, down to a Gabay–Toulouse like line. [17] To obtain this region one would need to also consider the 3D boundaries of the spin glass phase, and this is beyond the scope of the present paper. In any case, the AFM ordering will persist up to the line  $x = x_c$ .

At smaller defect concentrations, or at higher temperatures, i.e., for  $2\pi \gg t_0 > \lambda_0$ , Eqs. (51) and (60) give

$$\begin{aligned}
1 - \frac{\lambda_0}{t_N(x)} &= \left\{ 1 - \frac{3\lambda_0}{t_N(0)} \right\}^{1/3}, \\
\frac{1}{t_N(0)} &= \frac{1}{4\pi} \ln[\alpha(L_0 \tilde{C}(t_N(0), 0))^2]^{-1},
\end{aligned} \tag{62}$$

where  $t_N(0)$  is the Néel temperature of the pure antiferromagnet. The lowest order of this expression agrees with the results of Ref. [14], obtained by an annealed average.

## VI. ANNEALED AVERAGING

As stated above, the cuprates require some mixed annealed–quenched averaging. We start by reviewing a simple version of GI’s analysis. [14] In their approach,  $\mathbf{r}_\ell$  and  $\mathbf{a}(\mathbf{r}_\ell)$  are treated as quenched variables, with averages given by Eq. (5), while  $\mathbf{m}(\mathbf{r}_\ell)$  is treated as annealed. Thus, Eq. (6) is replaced by

$$[f_{i\mu}(\mathbf{r}_1) f_{j\nu}(\mathbf{r}_2)] = \delta_{ij} \delta(\mathbf{r}_{12}) \Lambda_{\mu\nu}(\mathbf{r}_1), \tag{63}$$

with

$$\Lambda_{\mu\nu}(\mathbf{r}) = m_\mu(\mathbf{r}) m_\nu(\mathbf{r}) M^2 x / d. \tag{64}$$

Initially,  $\mathcal{H}$  contains no interactions among the dipole moments  $\{\mathbf{m}(\mathbf{r})\}$ . However, the RG iterations generate the dipole–dipole interaction, as given by Eq. (28). This interaction is mediated via the canted background AFM moments. Treating this interaction as a small perturbation, to lowest order, we can next integrate the dipole moments out of the partition function, using the annealed averaging  $\langle m_\mu(\mathbf{r}_1) m_\nu(\mathbf{r}_2) \rangle = \delta_{\mu\nu} \delta(\mathbf{r}_{12}) / \mathcal{N}$ , so that

$$\langle \Lambda_{\mu\nu} \rangle = \delta_{\mu\nu} \Lambda \equiv \delta_{\mu\nu} M^2 x / (d\mathcal{N}). \tag{65}$$

Note that to this leading order,  $\Lambda = \lambda!$  GI wrote down a more general form for this thermal average, involving the susceptibility which results from the quadratic coupling in  $\mathcal{H}_{\text{dd}}$ . This reduces to the above expression at lowest order.

Up to Eq. (32), we have performed no averaging. In the annealed case, the recursion relations are derived from the same equations, using the averages as listed above. The

resulting recursion relation for  $1/t$  turns out to be the same as Eq. (34), with  $\lambda$  replaced by  $\Lambda$ . In contrast, the averaging over  $\mathbf{m}$  gives no contributions to the renormalization of  $\mathbf{f}_i$ , since all the generated terms which are linear in  $B_i^\mu$  involve odd powers of the  $u_i$ 's and the  $g_i^\mu$ 's, and therefore odd powers of the  $m_\mu$ 's. All of these vanish upon the annealed averaging over the  $m_\mu$ 's. Thus, we end up with

$$\left(\frac{\Lambda}{t^2}\right)' = b^{d-2}\left(\frac{\Lambda}{t^2}\right). \quad (66)$$

At 2D, Eq. (66) implies that  $\Lambda$  is unrenormalized. The solution of the recursion relation for  $t$  then yields

$$\ell = \frac{\pi}{\Lambda} \ln \frac{1 + 2\Lambda/t(0)}{1 + 2\Lambda/t(\ell)}. \quad (67)$$

Assuming that  $\Lambda \ll 2\pi$ , and integrating up to  $t(\ell^*) = 2\pi$ , yields

$$\ell^* \approx \frac{2\pi}{t(0)} \left(1 - \frac{\Lambda}{t(0)}\right), \quad (68)$$

which agrees to leading order with the quenched result (54).

This annealed averaging is legitimate as long as the renormalized distance between the impurities remains large, so that the dipole-dipole interaction which is generated during the iterations remains small. Note that the range of  $\mathcal{H}_{\text{dd}}$  is  $b = e^{\ell^*}$ . Thus, if  $e^{\ell^*}$  is small compared to the inter-impurity distance  $x^{-1/d}$ , then we can still treat the dipoles as independent degrees of freedom, ignore the interaction between them and continue the above annealed calculation. However, if  $e^{\ell^*}$  becomes larger than (but of the order of)  $x^{-1/d}$  then each renormalized cell contains more than one impurity, and the interaction between them comes into play. Since this interaction decays as  $1/r^d$ , the dipoles behave like a spin glass which is at its lower critical dimension. [17] Since the dipole-dipole energy is of order  $E_{\text{dd}} = \lambda\rho_s$ , we expect the dipole moments to develop spin-glassy correlations, with a correlation length  $\xi_{\text{sg}}$  which grows exponentially in  $E_{\text{dd}}/T$ . Since we showed that  $\xi_{2D}$  remains finite at all  $T$ , we expect that for  $T \ll E_{\text{dd}}$  one has  $\xi_{\text{sg}} \gg \xi_{2D}$ , the moments inside a renormalized cell (at distances smaller than  $\xi_{2D}$ ) freeze randomly, with the effective Edwards-Anderson order parameter

$Q$ , and we can switch to our quenched calculation. We thus choose to perform a prefacing annealed renormalization, up to  $e^{\ell_0} = L_0 \sim x^{-1/d}$ . For larger  $\ell$  we assume that the dipole moments are frozen at low  $T$ , and we switch to the quenched analysis of Secs. IV and V.

## VII. COMPARISON WITH EXPERIMENTS ON DOPED CUPRATES

Given the discussion in the previous section, we adopt the following strategy: We start by fitting  $A \equiv \lambda/x$  from the  $t$ -dependence of  $\xi_{2D}$  at high  $T$  and small  $x$ . As stated, this dependence is the same for both types of averages. Given  $A$ , we next fit the  $x$  dependence of  $\xi_{2D}$  in the limit of very low  $T$ , when  $\xi_{2D}$  is  $T$ -independent. This behavior should certainly be described by our quenched theory. The fit determines the pre-exponential factors. Finally, we use the results (without any further adjustments) to calculate the phase diagram,  $T_N(x)$ .

We begin with the temperature dependence of the correlation length at low concentrations,  $x < x_c$ . Data taken on a sample of  $\text{La}_2\text{CuO}_{4+\delta}$ , with  $T_N = 90\text{K}$ , [4] show a practically linear dependence of  $(t/2\pi) \ln(\xi/C)$  on  $1/t$ , in agreement with both our quenched result (54) and our annealed result (68). For the coefficient  $C$  in this fit we used  $C = 1.92\text{\AA}$ , derived from Eq. (56) with  $\rho_s = 24\text{meV}$  (See Ref. [4]) and  $L_0 = 1$ . The slope is  $\Lambda = \lambda_0 = 0.29(1)$  (see Fig. 1, and also Ref. [15]). To estimate the value of  $x$  for this sample, we follow Refs. [4] and [29] and approximate the line  $T_N(x)$  by the straight line  $T_N(x) \approx 325 - 16250x$ , which extrapolates to  $x = 0.02$  as  $T_N$  is extrapolated to zero. Using this approximation, we find that  $T_N = 90\text{K}$  at  $x = 0.0145$ . Thus,  $A = \lambda/x \approx 20$ . Although we have some problems with this linear extrapolation (see below), the value of  $x$  cannot be larger than  $x_c \approx 0.02$ , so the uncertainty in  $A$  is not more than 30%. Furthermore, although  $A$  might have a weak dependence on  $T$  and on  $x$ , this could most probably be absorbed in this error estimate. We thus use this estimate  $A = 20$  in everything that follows.

Keimer *et al.* [4] measured the temperature dependence of the correlation length for three magnetically disordered samples of  $\text{La}_{2-x}\text{Sr}_x\text{CuO}_4$ , with  $x \approx 0.02, 0.03$ , and  $0.04$ . The error in  $x$  is less than  $\sim 0.005$ . It is believed [4] that the hole concentration is about that of the

Sr ions. It was found that at low temperatures  $\xi$  does not depend on  $T$ , and falls with the increase of  $x$  faster than a power law. The  $\xi(T = 0)$  data is depicted in Fig. 2, together with the value of  $\xi$  cited in Ref. [12] for  $\text{La}_{1.95}\text{Ba}_{0.05}\text{CuO}_4$ . The figure also shows the theoretical values of  $\xi$ , calculated from Eq. (53), with  $L_0\tilde{C}(0, \lambda_0) = C_0\lambda_0^{\omega'}$ ,  $\lambda_0 = 20x$ ,  $C_0 = 2.8\text{\AA}$  and  $\omega' = 0.8$ . (In 2D, we now have  $\omega' = \omega - 1/2$ , from the  $x$  dependence of  $L_0$ ). We also reproduce in Fig. 2 the numerical results obtained in Ref. [27]. These authors computed the effect of holes localized on the oxygen atoms in the  $\text{CuO}_2$  plane. Their results, marked by ‘+’ in Fig. 2, are in agreement with our calculation.

We mention in passing that the correlation length at low temperature was also measured for  $x > 0.05$ . [30] These data were not included in our comparison, mainly because for these concentrations the holes are probably mobile.

We next turn to the temperature dependence of  $\xi$  at  $x > x_c$ . Figure 3 exhibits the calculated temperature dependence of  $\xi$ , for several concentrations  $x$ . The curves were found from Eq. (54) with  $C = L_0\tilde{C} = 1.92\text{\AA}$  ( $\lambda_0 < t_0$ , as in Fig. 1 discussed above), and from Eq. (53), with  $C(x) = 2.8\lambda_0^{0.8}\text{\AA}$  ( $\lambda_0 > t_0$ ). We have also used  $2\pi\rho_s = 150\text{ meV}$ . The theoretical lines are for  $x = 0.0225, 0.029$  and  $0.036$  (instead of the experimental values  $0.02, 0.03, \text{ and } 0.04$  given by Keimer *et al.*). The values chosen are within the experimental error. [4] Since the prefactors used in our fits differ in the limits  $\lambda_0 \ll t_0$  and  $\lambda_0 \gg t_0$ , the high- and low-temperature portions of the plots do not match at  $\lambda_0 = t_0$ . There the two segments are connected by dotted lines. The dashed lines in Fig. 3 represent the heuristic expression

$$\xi^{-1}(T, x) = \xi^{-1}(0, x) + \xi^{-1}(T, 0), \quad (69)$$

used in Ref. [4] to fit their data. It seems that the heuristic expression works as well; however, it seems that it has no theoretical basis.

The theoretical curves in Fig. 3 agree with the experimental results at temperatures lower than  $\sim 350 - 400\text{K}$ . At higher temperatures the calculated values of  $\xi$  are smaller than the measured ones. Perhaps, at such high temperatures thermal fluctuations come into play, causing a decrease of  $Q$  from  $1/\mathcal{N}$  to lower values. It is also possible that at high  $T$

the holes are more mobile, so that one should average over more than one bond per hole, thus reducing the effective dipole moment. At temperatures lower than 200 – 250 K the correlation length does not depend on the temperature up to exponentially small terms, of the order of  $\xi(0, T)^{-1}$ . [4] This nontrivial property of the correlation length is reproduced well by our calculation.

Given the above values for  $C_0$  and  $\omega$ , and the value  $\alpha = 10^{-4}$  from Ref. [4], we solved Eq. (61) and found the critical value of  $\lambda$  to be  $\lambda_c = 0.366$ . With  $A = 20$ , the critical concentration,  $x_c$ , for the disappearance of the long-range order at  $T = 0$  is found to be  $x_c = 0.0183$ , in very good agreement with the experimental value  $x_c = 0.0175$  from Ref. [5] (but in disagreement with Ref. [9], which gives  $x_c = .027$ ).

Using the above parameters, i.e.  $A = 20$ ,  $\alpha = 10^{-4}$ , and approximating the prefactor by a constant,  $C(t, x) \approx C(0, x_c) = C(0, 0.0183) = 1.26\text{\AA}$ , Fig. 4 shows the theoretical concentration dependence of  $T_N$ , calculated from Eqs. (62) for  $t_0 > \lambda_0$  and (61) for  $\lambda_0 > t_0$ , with no further fitting of the parameters. (The line  $t_0 = \lambda_0$  is also depicted in the figure.) At high temperatures the prefactor is larger,  $1.9\text{\AA}$ . However, the effect of this difference on  $T_N$  is small, since  $T_N$  depends on the prefactor only logarithmically. At small concentrations, our theoretical  $T_N(x)$  decreases with the increase of  $x$  linearly with the rate 55 K/% (based on the value of  $A$  as determined from the  $\xi$  data). At  $x = x_c$ ,  $T_N(x_c)$  is roughly equal to  $T_N(0)/3$ . Then  $T_N$  abruptly falls to zero, as our calculation finds that the correlation length is independent of the temperature for  $t_0 < \lambda_0$ .

Figure 4 includes the results of several experiments. It is seen that those of Ref. [29] seem to disagree with our phase diagram: the data fall linearly with a slope of 162 K/%, (larger by about a factor of 3 than our theoretical value, which was extracted from the data for  $\xi$ ), extrapolating to  $x = .02$  without the jump in  $T_N$ . However, we should note that Chen *et al.* [29] determined  $x$  for their O-doped samples from Hall effect data. In Ref. [31]  $T_N$  and the Hall density of holes were measured for a Sr doped sample. The Sr concentration in the melt was 0.0022, while the Hall measurements gave a smaller hole density, 0.0016. Figure 4 shows that in this case the experimental point (with  $x = 0.0022$ ) is closer to the

theoretical curve than the data from Ref. [29]. Saylor and Hohenemser [6] measured  $T_N(x)$  in Sr-doped samples of lanthanum cuprate. Although their  $T_N(0) = 317$  K was somewhat less than in the best samples of Ref. [4], their  $T_N(x)$  decreased linearly with the rate 90 K/% till  $x = 0.015$ . In the region between  $x = 0.015$  and 0.018,  $T_N$  fell from  $\approx 180$  K to 20 K. This behavior of  $T_N(x)$  is close to our phase diagram, Fig. 4.

Very recently, Wakimoto *et al.* [10] measured the phase diagram of oxygen doped  $\text{La}_{1.95}\text{Bi}_{0.05}\text{CuO}_4$ , and their  $T_N(x)$  agrees qualitatively with our theory: it falls almost linearly down to  $T_N(0.012) \approx 160$  K, and then drops sharply towards  $x_c \approx 0.015$ . Both this small value of  $x_c$  and the low- $T$  value of the correlation length near  $x_c$ , as measured in Ref. [10], are consistent with our calculations, with  $A \approx 30$ .

### VIII. DISCUSSION

Most of this paper was devoted to a detailed description of the theory for the effects of FM bonds on AFM correlations in doped antiferromagnets. We hope that this will stimulate some material research onto such systems. It is also hoped that this exact solutions could be used to study more systems with correlated random fields.

In the previous section we discussed some fits of our theory (with both annealed and quenched averaging) to data from doped lamellar oxides. As stated in the Introduction, these fits are based on various assumptions, and thus deserve some further discussion. Hopefully, the reader is already convinced that our fits give a nice interpolation between the annealed and quenched calculations, for high and low temperatures respectively. We now discuss possible problems in using our model of localized holes for these systems.

First of all, we note that experiments on both O-doped and Sr-doped  $\text{La}_2\text{CuO}_4$  indicate a localization length of the hole of order of two lattice constants. [29,31] Furthermore, for Sr-doping, the hole moves around the center of a Cu-plaquette, and this might imply a quadrupolar behavior, rather than a dipolar one, for the spin canting. [15] However, there are arguments in the literature, [32] claiming that holes which move around such a center



create Skyrmion-type distortions of the AFM background, decaying as  $1/r$ . Thus, our calculation may remain qualitatively correct, although we might have to use a different expression for our parameter  $A$ . We might also add that to linear order in  $x$  one effectively considers only single impurities, and therefore mobile and static holes will have the same (classical) effects. Since  $A$  is fitted from the experiments anyway, it could result from any of the above cases.

Another alternative is to abandon the localized picture altogether. The effects of *mobile* holes on the AFM correlations were considered in many papers. One approach [33] concluded that mobile holes drive the system to the quantum disordered state. Indeed, we solved the *classical* NL $\sigma$ M, and thus ignored quantum fluctuations. However, for the undoped systems the classical expressions described the exponential factor of the correlation length rather well. [19,4] We have checked that integration of the quantum fluctuations, similar to that done in Ref. [19], only renormalizes the initial parameters of the effective classical model also in the random case.

Another approach [34] proposed that the AFM order is destroyed by the segregation of holes into striped phases. In view of the experiments mentioned above, which show that the holes are localized (and the conductivity obeys the variable range hopping law) at low  $T$  and low  $x$ , we believe that these alternative approaches should be used only for  $x > 5\%$ , or at higher  $T$ . Indeed, to our knowledge there is little experimental evidence that stripes exist at  $x < 5\%$ , or that quantum fluctuations were observed at low  $T$  in that range. However, we cannot rule out some crossover from our localized to the mobile behavior at the metal-insulator transition (around  $x = 5\%$  and at higher  $T$ ). In any case, it would be nice to find more experimental tests that would distinguish between the various scenarios for the cuprates.

## ACKNOWLEDGMENTS

We have benefitted from many discussions with R. J. Birgeneau , A. B. Harris, A. S. Ioselevich, M. A. Kastner, D. E. Khmel'nitskii, V. V. Lebedev, T. Nattermann and M. Schwartz. This project has been supported by a grant from the U. S.–Israel Binational Science Foundation (BSF).

## APPENDIX A: GAUGE TRANSFORMATION OF THE FIELDS $\phi_\mu$

In order to eliminate the functions  $A_i^{\mu\nu}(\mathbf{r})$  from the expression for the derivatives  $\partial_i \tilde{\mathbf{n}}$  [Eq. (15)] we introduce the transformation

$$\phi_\mu = \sum_{\mu_1} T_{\mu\mu_1} \tilde{\phi}_{\mu_1}, \quad (\text{A1})$$

where the coefficients  $T_{\mu\mu_1}$  are determined by

$$\partial_i T_{\mu\mu_1} = \sum_{\mu_2} A_i^{\mu\mu_2} T_{\mu_2\mu_1}, \quad (\text{A2})$$

with

$$\sum_{\mu} T_{\mu\mu_1} T_{\mu\mu_2} = \delta_{\mu_1\mu_2}, \quad T_{\mu\mu_1} = T_{\mu_1\mu}. \quad (\text{A3})$$

Note that the sums run from 1 to  $\mathcal{N} - 1$ . Assuming that  $A_i^{\mu\mu_1}$  is independent of  $x_i$ , the solution of Eqs. (A2) and (A3) reads  $T_{\mu\mu_1} = T_{\mu\mu_1}^0 \exp(-i\kappa x_i)$ , where  $\kappa$  is a real eigenvalue of the Hermitian matrix  $iA_i$ . Deviations from this approximation naturally involve higher derivatives of  $A_i^{\mu\mu_1}$  which are related to higher powers of the gradients in  $\mathcal{H}$ . These are strongly irrelevant.

Inserting the above relations into Eq. (15) we obtain

$$\begin{aligned} \partial_i \mathbf{n} = & \tilde{\mathbf{n}} \left[ \partial_i \sqrt{1 - \tilde{\phi}^2} - \sum_{\mu} \tilde{\phi}_{\mu} \sum_{\nu} T_{\nu\mu} B_i^{\nu} \right] \\ & + \sum_{\mu} \left[ B_i^{\mu} \mathbf{e}_{\mu} \sqrt{1 - \tilde{\phi}^2} + \partial_i \tilde{\phi}_{\mu} \sum_{\nu} T_{\nu\mu} \mathbf{e}_{\nu} \right]. \end{aligned} \quad (\text{A4})$$

Therefore, defining

$$\tilde{\mathbf{e}}_\mu = \sum_\nu \mathbf{e}_\nu T_{\nu\mu}, \quad \tilde{B}_i^\mu = \sum_\nu B_i^\nu T_{\nu\mu}, \quad (\text{A5})$$

Eq. (A4) takes the form of Eq. (15) without the  $A_i^{\nu\mu}$  terms, with  $\phi_\mu$ ,  $\mathbf{e}_\mu$  and  $B_i^\mu$  replaced by  $\tilde{\phi}_\mu$ ,  $\tilde{\mathbf{e}}_\mu$  and  $\tilde{B}_i^\mu$ , respectively. For brevity, we have omitted in the subsequent derivations the superscript  $\tilde{\phantom{x}}$ . It is seen that the gauge transformation can be regarded as a rotation of the base vectors  $\mathbf{e}_\mu$ , and reflects the arbitrariness of their choice. [24]

## APPENDIX B: THE PHASE BOUNDARY AT $2+\epsilon$ DIMENSIONS

For completeness, we present here the solution of the recursion relations (46) in  $d = 2 + \epsilon$  dimensions, and obtain the critical line  $t_N(x)$ , where  $x$  is the defect concentration.

The recursion relations (46) have four fixed points in the  $[\lambda, t]$  plane:  $[0, 0]$ ,  $[0, 2\pi\epsilon/(\mathcal{N} - 2)]$ ,  $[2\pi\epsilon/\mathcal{N}, 0]$ , and  $[2\pi\epsilon/(2\mathcal{N} - 3), 2\pi\epsilon/(2\mathcal{N} - 3)]$ . For  $\mathcal{N} > 3/2$ , the first point is stable, the last one is doubly unstable and the other two are unstable in one direction and stable in the other.

The solution of Eqs. (46) for  $\ell > \ell_0$  and Heisenberg spins ( $\mathcal{N} = 3$ ) reads

$$\begin{aligned} \lambda(\ell) &= \lambda_0 \left[ e^{\epsilon(\ell-\ell_0)} - \frac{3\lambda_0}{2\pi\epsilon} (e^{\epsilon(\ell-\ell_0)} - 1) \right]^{-1}, \\ \frac{1 - \lambda(\ell)/t(\ell)}{1 - \lambda_0/t_0} &= \left[ \frac{\lambda(\ell) - 2\pi\epsilon/3}{\lambda_0 - 2\pi\epsilon/3} \right]^{1/3}. \end{aligned} \quad (\text{B1})$$

The phase boundary is identified as the line which separates the flow to the origin (in the ordered phase) from the flow to infinity (in the disordered phase). It is easy to check that for  $t_0 > \lambda_0$ , the initial point  $[\lambda_0, t_0]$  will flow to the ‘‘pure’’ fixed point  $[0, 2\pi\epsilon]$  when

$$\begin{aligned} 1 - \frac{\lambda_0}{t_N(x)} &= \left( 1 - \frac{3\lambda_0}{2\pi\epsilon} \right)^{1/3}, \\ 0 \leq \lambda_0 \leq \lambda_c &= \frac{2\pi\epsilon}{3}, \end{aligned} \quad (\text{B2})$$

where the second of Eqs. (B1) has been used. On the other hand, using again that equation, we find that for  $t_0 < \lambda_0$  the solution flows to the ‘‘random’’ fixed point,  $[2\pi\epsilon/3, 0]$ , provided that

$$\lambda_0 \equiv \lambda_c = \frac{2\pi\epsilon}{3}, \quad \lambda_c > t_0 > 0. \quad (\text{B3})$$

The two portions of the critical line, Eqs. (B2) and (B3), are separated by the multicritical point at  $[2\pi\epsilon/3, 2\pi\epsilon/3]$ . It is interesting to note that also here, like the behavior found for  $t_N(x)$  for weakly coupled planes, there is a vertical section of the phase boundary.

We thus conclude that for  $t_0 > \lambda_0$  the randomness is irrelevant, and the “pure” critical behavior (which has a correlation length exponent  $\nu = 1/\epsilon$ ) remains stable. However, finite values of  $\lambda$  yield a correction to this behavior, with exponent  $-\epsilon$  (or, more generally,  $-\epsilon/(\mathcal{N}-2)$ ). The correlation length is obtained from Eq. (48), using the matching conditions (49). One finds

$$\xi \sim \exp(\ell^*) = L_0 \left[ \frac{\lambda^{-1}(\ell^*) - \lambda_c^{-1}}{\lambda_0^{-1} - \lambda_c^{-1}} \right]^{1/\epsilon}. \quad (\text{B4})$$

For  $t_0 > \lambda_0$  the iterations are stopped at  $t(\ell^*) \sim 2\pi$ . In the range  $\lambda(\ell^*) < \lambda_c$  we can find  $\lambda(\ell^*)$  by considering the difference  $\lambda_0/t_N - \lambda_0/t_0$ , using Eqs. (B1) and (B2). We find

$$t_N^{-1} - t_0^{-1} \simeq \lambda_0^{-1} \frac{\lambda(\ell^*)}{3\lambda_c} \left(1 - \frac{\lambda_0}{\lambda_c}\right)^{1/3}, \quad (\text{B5})$$

from which it follows that

$$\begin{aligned} \xi \sim e^{\ell^*} &\sim (t_0 - t_N(x))^{-1/\epsilon} \times \\ &[1 + Bx(t_0 - t_N(x)) + \dots], \end{aligned} \quad (\text{B6})$$

where  $B$  is a constant and the term associated with it comes from corrections of order  $\lambda_0 e^{-\ell^*}$ .

For  $\lambda_0 > t_0$ ,  $\lambda(\ell^*) = 2\pi$ , so that

$$\xi \sim e^{\ell^*} \sim (\lambda_0^{-1} - \lambda_c^{-1})^{-1/\epsilon}. \quad (\text{B7})$$

## REFERENCES

- [1] J. Villain, Z. Phys. B**33**, 31 (1979).
- [2] A. Aharony, R. J. Birgeneau, A. Coniglio, M. A. Kastner, and H. E. Stanley, Phys. Rev. Lett. **60**, 1330 (1988).
- [3] R. J. Birgeneau and G. Shirane, in *Physical Properties of High Temperature Superconductors*, D. M. Ginzberg, ed., (World Scientific, Singapore, 1989).
- [4] B. Keimer, N. Belk, R. J. Birgeneau, A. Cassanho, C. Y. Chen, M. Greven, M. A. Kastner, A. Aharony, Y. Endoh, R. W. Erwin, and G. Shirane, Phys. Rev. B**46**, 14 034 (1992).
- [5] G. Shirane, R. J. Birgeneau, Y. Endoh, and M. A. Kastner, Physica B **197**, 158 (1994).
- [6] J. Saylor and C. Hohenemser, Phys. Rev. Lett. **22**, 1824 (1990).
- [7] J. H. Cho, F. C. Chou, and D. C. Johnston, Phys. Rev. Lett. **70**, 222 (1993).
- [8] F. C. Chou, F. Borsa, J. H. Cho, D. C. Johnston, A. Lascialfari, D. R. Torgeson, and J. Ziolo, Phys. Rev. Lett. **71**, 2323 (1993).
- [9] H. Kageyama, K. Yoshimura, M. Kato, and K. Kosuge, J. Phys. Soc. Jpn. **64**, 2144 (1995).
- [10] S. Wakimoto, K. Kurahashi, C. H. Lee, K. Yamada, Y. Endoh, and S. Hosoya, Physica B **237-238**, 91 (1997).
- [11] F. C. Chou, N. R. Belk, M. A. Kastner, R. J. Birgeneau, and A. Aharony, Phys. Rev. Lett. **75**, 2204 (1995) and references therein.
- [12] S. H. Hayden, G. Appeli, H. Mook, D. Rytz, M. F. Hundley, and Z. Fisk, Phys. Rev. Lett. **66**, 821 (1991).
- [13] Ch. Niedermayer, C. Bernhard, T. Blasius, A. Golnik, A. Moodenbaugh and J. I. Bud-

- nick, Phys. Rev. Lett. **80**, 3843 (1998).
- [14] L. I. Glazman and A. S. Ioselevich, Z. Phys. **B80**, 133 (1990).
- [15] I. Ya. Korenblit, Phys. Rev. **B51**, 12 551 (1995).
- [16] K. Binder and A. P. Young, Rev. Mod. Phys. **58**, 80 (1986).
- [17] K. H. Fischer and J. A. Hertz, *Spin Glasses* (Cambridge University Press, 1991).
- [18] P. Lacour-Gayet and G. Toulouse, J. Physique **35**, 425 (1974) .
- [19] S. Chakravarty, B. I. Halperin, and D. R. Nelson, Phys. Rev. **B39**, 2344 (1989).
- [20] Y. Imry and S. K. Ma, Phys. Rev. Lett. **35**, 1399 (1975).
- [21] E. Brézin and J. Zinn-Justin, Phys. Rev. **B14**, 3110 (1976).
- [22] D. R. Nelson and R. A. Pelcovits, Phys. Rev. **B16**, 2191 (1977).
- [23] D. S. Fisher, Phys. Rev. **B31**, 7233 (1985).
- [24] A. M. Polyakov, Phys. Lett. **B59**, 79 (1975); *Gauge Fields and Strings*, in Contemporary Concepts in Physics, H. Feshbach, ed., (Harwood Academic, 1987).
- [25] V. L. Berezinskii and A. Ya. Blank, Sov. Phys. JETP **37**, 369 (1973).
- [26] A. Z. Patashinskii and V. L. Pokrovskii, *Fluctuation Theory of Phase Transitions* (Pergamon Press, Oxford, 1979).
- [27] R. J. Gooding and A. Mailhot, Phys. Rev. **B44**, 11 852 (1991).
- [28] P. Hasenfranz and F. Nidermayer, Phys. Lett. **B268**, 231 (1991).
- [29] C. Y. Chen, R. J. Birgeneau, M. A. Kastner, N. W. Preyer, and T. Thio, Phys. Rev. **B43**, 392 (1991).
- [30] R. J. Gooding, N. M. Salem, R. J. Birgeneau, and F. C. Chou, Phys. Rev. **B55**, 6360 (1997) and references therein.

- [31] C. Y. Chen, E. C. Branlund, ChinSung Bae, K. Yang, M. A. Kastner, A. Cassanho, and R. J. Birgeneau, *Phys. Rev.* **B51**, 3671 (1995).
- [32] B. Shraiman and E. D. Siggia, *Phys. Rev.* **B42**, 2485 (1990). See also V. L. Pokrovsky and G. V. Uimin, *Physica C* **160**, 323 (1989); R. J. Gooding, *Phys. Rev. Lett.* **66**, 2266 (1991); R. J. Gooding, N. M. Salem and A. Mailhot, *Phys. Rev.* **B49**, 6067 (1994) and Ref. [27].
- [33] A. V. Chubukov *et al.*, *Phys. Rev.* **B49**, 11 919 (1994); S. Sachdev, *Phys. Rev.* **B49**, 6770 (1994).
- [34] A. H. Castro Neto and D. Hone, *Phys. Rev. Lett.* **76**, 2165 (1996).

# FIGURES

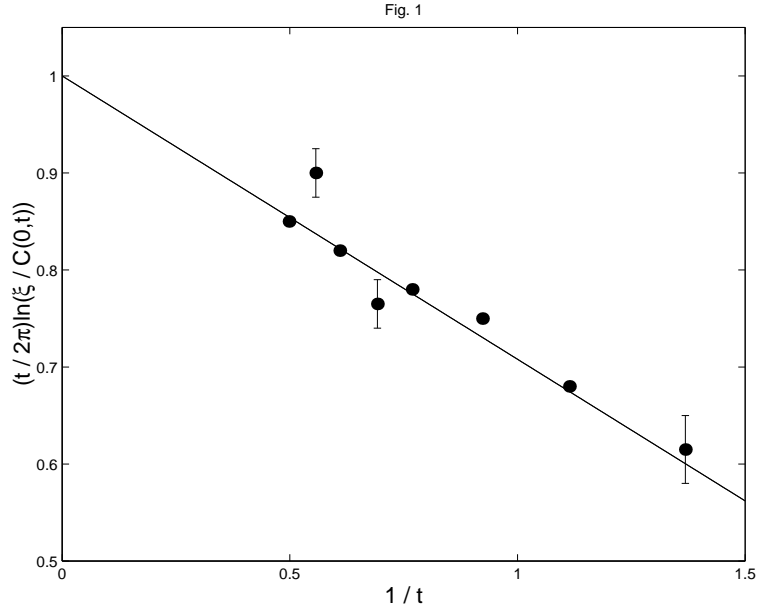


FIG. 1.  $(t/2\pi)\ln(\xi/C)$  versus  $1/t$  for  $\text{La}_2\text{CuO}_{4+\delta}$  with  $T_N = 90\text{K}$ . The points are from Ref. 4. The straight line shows the fit to Eq. (54), with  $\lambda_0/t_0 \ll 1$ .

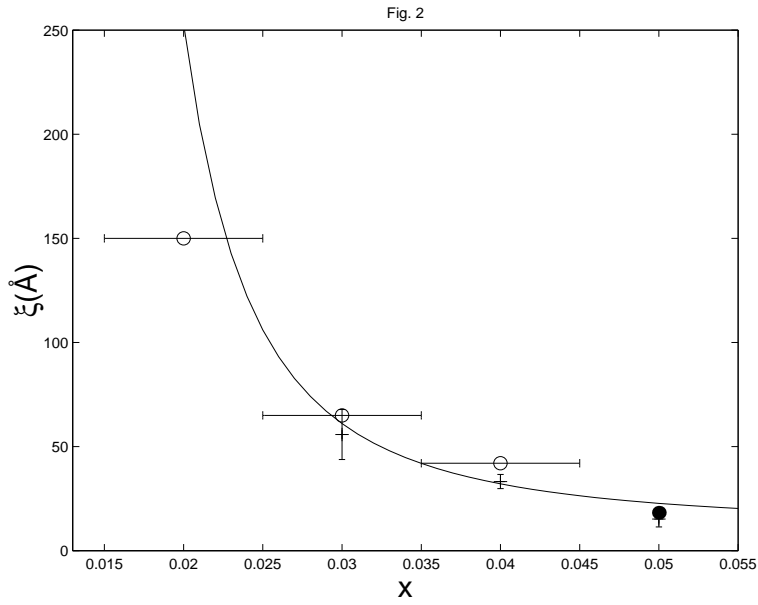




FIG. 2. Dependence of  $\xi_{2D}$  at  $T = 0$  on  $x$ . The empty<sup>4</sup> and full<sup>12</sup> circles indicate experiments, +’s show numerical simulation<sup>27</sup> data. The solid line represents  $2.8\lambda^{0.8}\text{\AA}\exp(2\pi/3\lambda)$ , with  $\lambda = 20x$ .

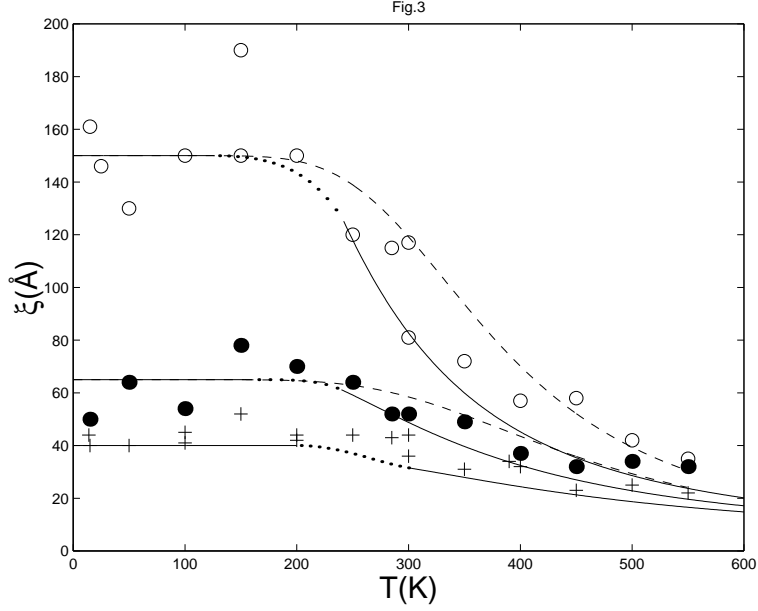


FIG. 3. Dependence of  $\xi_{2D}(t, \lambda)$  on  $T$  for several concentrations. Symbols are from experiments: empty circles for  $x = 0.02$ , full circles for  $x = 0.03$ , +’s for  $x = 0.04$ , all from Ref. 4. Full lines show results from Fig. 2 (for low  $T$ ) or Eq. (54), with  $C = L_0\tilde{C} = 1.92\text{\AA}$  (for high  $T$ ). Dotted lines interpolate between these low- and high- $T$  theories. Dashed lines correspond to Eq. (69).

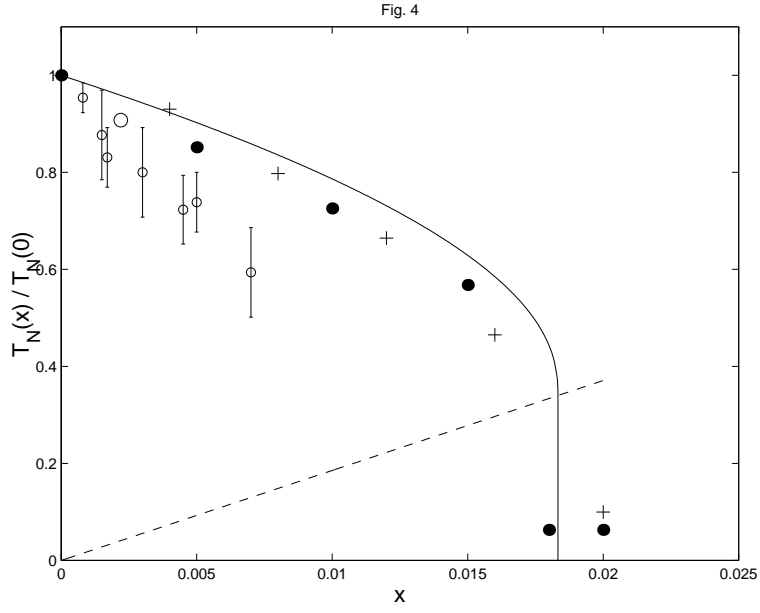


FIG. 4.  $T_N(x)/T_N(0)$  versus  $x$ . Full line is theory, and the points are from experiments: full circles from Ref. 6 , +’s from Ref. 7, empty circles from Refs. 29 and 31. Dashed line indicates  $\lambda_0 = t_0$ .